

# Chopper-Stabilized, Two-Wire Hall-Effect Switches

## FEATURES AND BENEFITS

- AEC-Q100 automotive qualified
- High-speed, 4-phase chopper stabilization
- Low switchpoint drift throughout temperature range
- Low sensitivity to thermal and mechanical stresses
- On-chip protection
  - Supply transient protection
  - Reverse-battery protection
  - On-board voltage regulator
  - 3 to 24 V operation
- Solid-state reliability
- Robust EMC and ESD performance
- Industry-leading ISO 7637-2 performance through use of proprietary, 40 V clamping structures

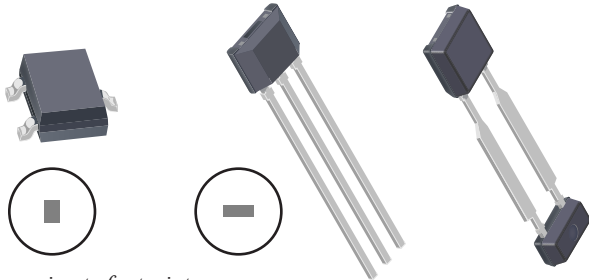
*Continued on the next page...*

## PACKAGES

**3-pin SOT23-W**  
2 mm × 3 mm × 1 mm (suffix LH)

**3-pin ultramini SIP**  
1.5 mm × 4 mm × 3 mm (suffix UA)

**2-pin ultramini SIP**  
1.5 mm × 4 mm × 4 mm (suffix UB)



*Approximate footprint*

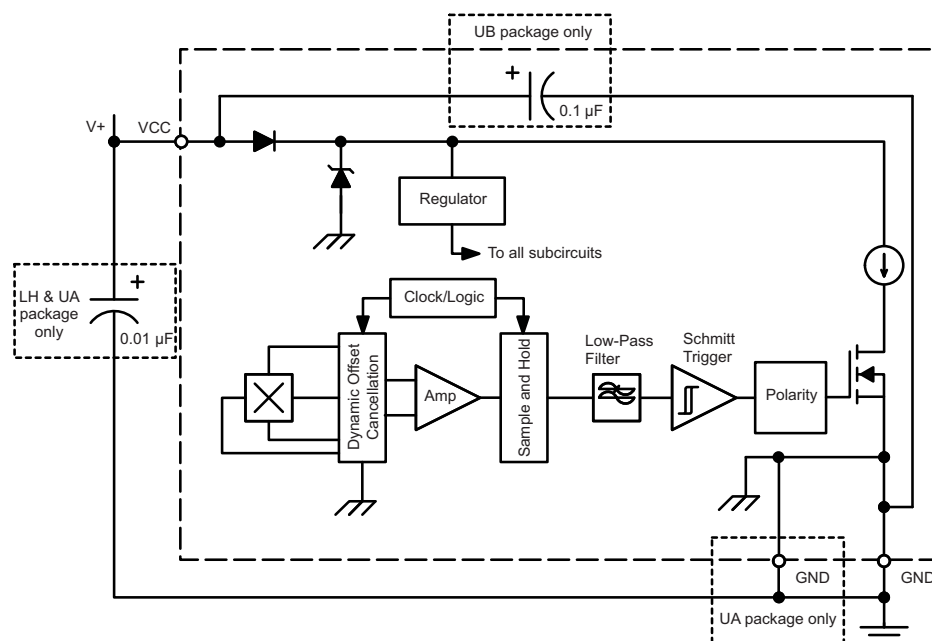
## DESCRIPTION

The A1150, A1152, A1153, A1155, A1156, A1157, and A1158 comprise a family of two-wire, unipolar, Hall-effect switches, which are factory-trimmed to optimize magnetic switchpoint accuracy. These devices are produced on the Allegro™ advanced BiCMOS wafer fabrication process, which implements a high-frequency, 4-phase, chopper-stabilization technique. This technique achieves magnetic stability over the full operating temperature range, and eliminates offsets inherent in devices with a single Hall element that are exposed to harsh application environments.

The A115x family has a number of automotive applications. These include sensing seat track position, seat belt buckle presence, hood/trunk latching, and shift selector position.

Two-wire unipolar switches are particularly advantageous in cost-sensitive applications because they require one less wire for operation versus the more traditional open-collector output switches. Additionally, the system designer inherently gains diagnostics because there is always output current flowing, which should be in either of two narrow ranges. Any current level not within these ranges indicates a fault condition.

All family members are offered in three package styles. The LH is a SOT-23W style, miniature, low profile package for surface-mount applications. The UA is a 3-pin, ultra-mini, single inline package (SIP) for through-hole mounting. The UB is a 2-pin, ultra-mini, single inline package (SIP) for through-hole mounting. All three packages are lead (Pb) free, with 100% matte-tin leadframe plating.



**Functional Block Diagram**

**FEATURES AND BENEFITS (continued)**

- Extended Operating Ambient temperature range, –40°C to 150°C
- UB package with integrated 0.1  $\mu$ F bypass capacitor



**SELECTION GUIDE**

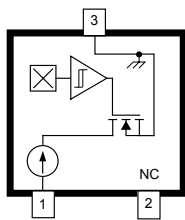
Part Number	Packing	Package	Output ( $I_{CC}$ ) in South Polarity Field	Supply Current at $I_{CC(L)}$ (mA)	Magnetic Operate Point, $B_{OP}$ (G)
A1150LLHLX-T	13-in. reel, 10 000 pieces/reel	3-pin SOT23W surface mount	Low	2 to 5	50 to 110
A1150LUA-T	Bulk, 500 pieces/bag	3-pin SIP through hole			
A1152LLHLX-T	13-in. reel, 10 000 pieces/reel	3-pin SOT23W surface mount	Low	5 to 6.9	
A1152LUA-T	Bulk, 500 pieces/bag	3-pin SIP through hole			
A1152LUBTN-T	13-in. reel, 4 000 pieces/reel	2-pin SIP through hole			
A1153LLHLX-T	13-in. reel, 10 000 pieces/reel	3-pin SOT23W surface mount	High	5 to 6.9	
A1153LUA-T	Bulk, 500 pieces/bag	3-pin SIP through hole			
A1153LUBTN-T	13-in. reel, 4 000 pieces/reel	2-pin SIP through hole			
A1155LLHLX-T	13-in. reel, 10 000 pieces/reel	3-pin SOT23W surface mount	Low	5 to 6.9	20 to 60
A1155LUA-T	Bulk, 500 pieces/bag	3-pin SIP through hole			
A1155LUBTN-T	13-in. reel, 4 000 pieces/reel	2-pin SIP through hole			
A1156LLHLX-T	13-in. reel, 10 000 pieces/reel	3-pin SOT23W surface mount	High	5 to 6.9	
A1156LUA-T	Bulk, 500 pieces/bag	3-pin SIP through hole			
A1156LUBTN-T	13-in. reel, 4 000 pieces/reel	2-pin SIP through hole			
A1157LLHLX-T	13-in. reel, 10 000 pieces/reel	3-pin SOT23W surface mount	Low	2 to 5	20 to 80
A1157LLHLT-T	7-in. reel, 3000 pieces/reel	3-pin SOT23W surface mount			
A1157LUA-T	Bulk, 500 pieces/bag	3-pin SIP through hole			
A1158LLHLX-T	13-in. reel, 10 000 pieces/reel	3-pin SOT23W surface mount	High		
A1158LLHLT-T	7-in. reel, 3000 pieces/reel	3-pin SOT23W surface mount			
A1158LUA-T	Bulk, 500 pieces/bag	3-pin SIP through hole			

## SPECIFICATIONS

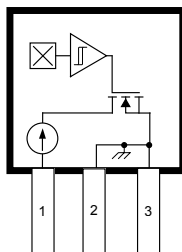
### ABSOLUTE MAXIMUM RATINGS

Characteristic	Symbol	Notes	Rating	Unit
Forward Supply Voltage	$V_{CC}$		28	V
Reverse Supply Voltage	$V_{RCC}$		-18	V
Magnetic Flux Density	B		Unlimited	G
Operating Ambient Temperature	$T_A$	Range L	-40 to 150	°C
Maximum Junction Temperature	$T_{J(max)}$		165	°C
Storage Temperature	$T_{stg}$		-65 to 170	°C

### PINOUT DIAGRAMS AND TERMINAL LIST TABLE



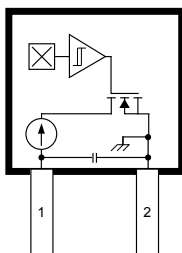
LH Package [1]



UA Package

#### LH and UA Terminal List Table

Number	Name		Function
	LH package	UA package	
1	VCC	VCC	Input power supply
2	NC	GND	LH package: no connection, it is highly recommended that this pin be tied to GND [1] UA package: ground terminal
3	GND	GND	Ground terminal



UB Package

#### UB Terminal List Table

Number	Name	Function
1	VCC	Input power supply
2	GND	Ground terminal

[1] Package style LH pin 2 is not internally connected to the IC ground and therefore should not be used as a ground reference pin. For maximum EMC and ESD robustness it is highly recommended that this pin be tied to ground.

**ELECTRICAL CHARACTERISTICS: Valid at  $T_A = -40^\circ\text{C}$  to  $150^\circ\text{C}$ ,  $T_J < T_J(\text{max})$ ,  $C_{\text{BYP}} = 0.01 \mu\text{F}$ , through operating supply voltage range, unless otherwise noted**

Characteristics	Symbol	Test Conditions		Min.	Typ.	Max.	Unit
Supply Voltage [1][2]	$V_{\text{CC}}$	Operating, $T_J \leq 165^\circ\text{C}$		3.0	–	24	V
Supply Current	$I_{\text{CC(L)}}$	A1150, A1157	$B > B_{\text{OP}}$	2.0	–	5.0	mA
		A1158	$B < B_{\text{RP}}$				
		A1152, A1155	$B > B_{\text{OP}}$	5	–	6.9	mA
		A1153, A1156	$B < B_{\text{RP}}$				
	$I_{\text{CC(H)}}$	A1150, A1152, A1155, A1157	$B < B_{\text{RP}}$	12	–	17	mA
	A1153, A1156, A1158	$B > B_{\text{OP}}$					
Supply Zener Clamp Voltage	$V_{\text{Z(sup)}}$	$I_{\text{CC(L)(max)}} + 3 \text{ mA}$ , $T_A = 25^\circ\text{C}$		28	–	–	V
Supply Zener Clamp Current	$I_{\text{Z(sup)}}$	$V_{\text{Z(sup)}} = 28 \text{ V}$		–	–	$I_{\text{CC(L)(max)}} + 3 \text{ mA}$	mA
Reverse Supply Current	$I_{\text{RCC}}$	$V_{\text{RCC}} = -18 \text{ V}$		–	–	-1.6	mA
Output Slew Rate [3]	di/dt	LH and UA	No bypass capacitor, capacitance of probe $C_S = 20 \text{ pF}$	–	90	–	mA/ $\mu\text{s}$
		UB	Integrated bypass capacitor, capacitance of probe $C_S = 20 \text{ pF}$	–	0.22	–	mA/ $\mu\text{s}$
Chopping Frequency	$f_c$			–	700	–	kHz
Power-Up Time [4][5]	$t_{\text{on}}$	A1150, A1152, A1155, A1157	$B > B_{\text{OP}} + 10 \text{ G}$	–	–	25	$\mu\text{s}$
		A1153, A1156, A1158	$B < B_{\text{RP}} - 10 \text{ G}$				
Power-Up State [2][4][6][7]	POS	$t_{\text{on}} < t_{\text{on(max)}}$ , $V_{\text{CC}}$ slew rate $> 25 \text{ mV}/\mu\text{s}$		–	$I_{\text{CC(H)}}$	–	–

[1]  $V_{\text{CC}}$  represents the generated voltage between the VCC pin and the GND pin.

[2] The  $V_{\text{CC}}$  slew rate must exceed 600 mV/ms from 0 to 3 V. A slower slew rate through this range can affect device performance.

[3] Measured without bypass capacitor between VCC and GND. Use of a bypass capacitor results in slower current change.

[4] Power-Up Time is measured without and with bypass capacitor of 0.01  $\mu\text{F}$ . Adding a larger bypass capacitor would cause longer Power-Up Time.

[5] Guaranteed by characterization and design.

[6] Power-Up State as defined is true only with a  $V_{\text{CC}}$  slew rate of 25 mV/ $\mu\text{s}$  or greater.

[7] For  $t > t_{\text{on}}$  and  $B_{\text{RP}} < B < B_{\text{OP}}$ , Power-Up State is not defined.

**MAGNETIC CHARACTERISTICS [1]: Valid at  $T_A = -40^\circ\text{C}$  to  $150^\circ\text{C}$ ,  $T_J < T_J(\text{max})$ , unless otherwise noted**

Characteristics	Symbol	Test Conditions		Min.	Typ.	Max.	Unit [2]
Magnetic Operating Point	$B_{\text{OP}}$	A1150, A1152, A1153		50	–	110	G
		A1155, A1156		20	–	60	G
		A1157, A1158		20	–	80	G
Magnetic Release Point	$B_{\text{RP}}$	A1150, A1152, A1153		45	–	105	G
		A1155, A1156		10	–	55	G
		A1157, A1158		10	–	60	G
Hysteresis	$B_{\text{HYS}}$			5	–	30	G

[1] Relative values of B use the algebraic convention, where positive values indicate south magnetic polarity, and negative values indicate north magnetic polarity; therefore greater B values indicate a stronger south polarity field (or a weaker north polarity field, if present).

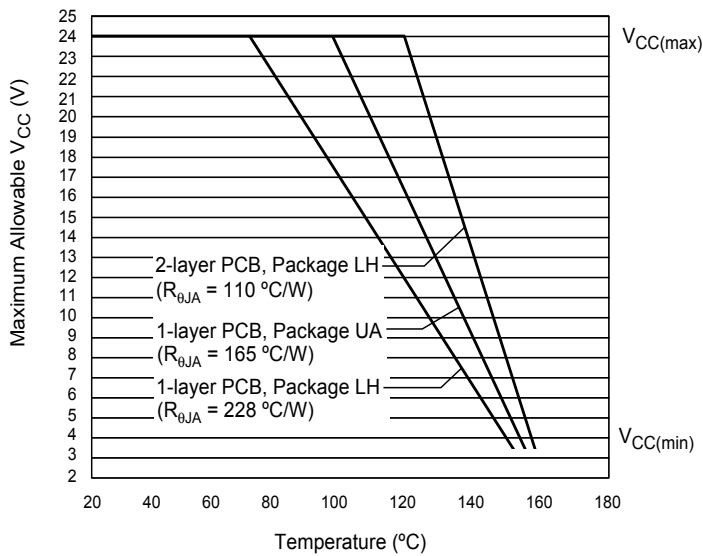
[2] 1 G (gauss) = 0.1 mT (millitesla).

**THERMAL CHARACTERISTICS:** may require derating at maximum conditions; see application information

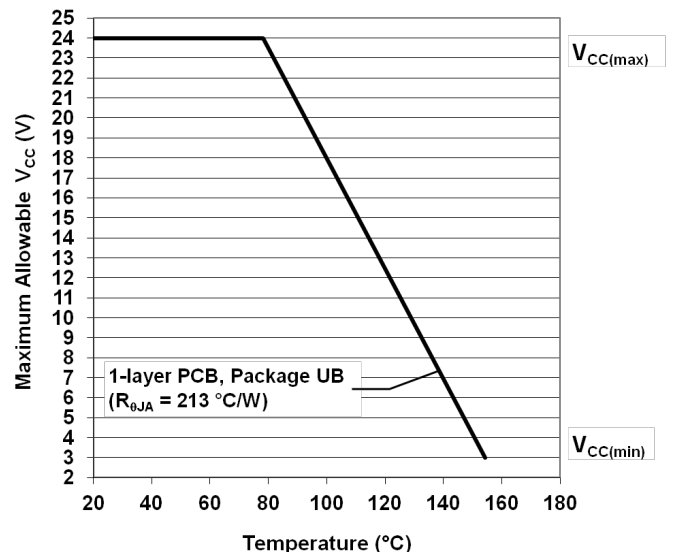
Characteristic	Symbol	Test Conditions*	Value	Unit
Package Thermal Resistance	$R_{\theta JA}$	Package LH, on 1-layer PCB with copper limited to solder pads	228	$^{\circ}\text{C}/\text{W}$
		Package LH, on 2-layer PCB with 0.463 in. <sup>2</sup> of copper area each side	110	$^{\circ}\text{C}/\text{W}$
		Package UA, on 1-layer PCB with copper limited to solder pads	165	$^{\circ}\text{C}/\text{W}$
		Package UB, on 1-layer PCB with copper limited to solder pads	213	$^{\circ}\text{C}/\text{W}$

\*Additional thermal information available on the Allegro website

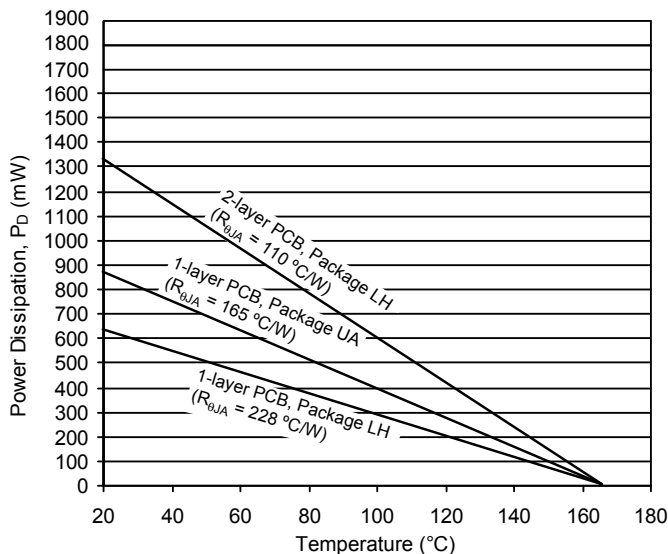
**LH and UA Power Derating Curve**



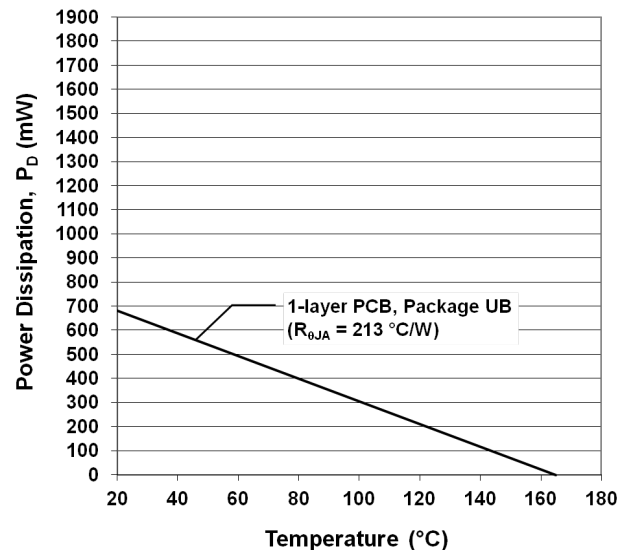
**UB Power Derating Curve**



**LH and UA Power Dissipation versus Ambient Temperature**

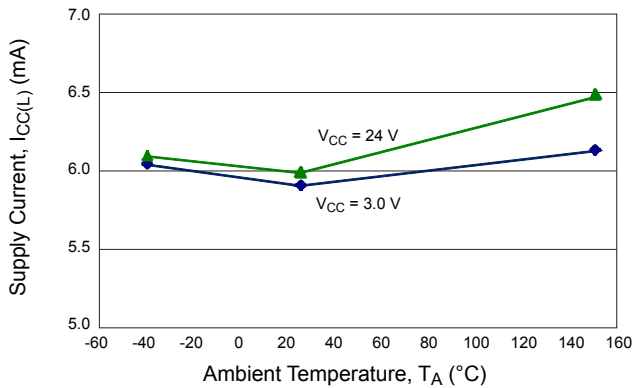


**UB Power Dissipation versus Ambient Temperature**

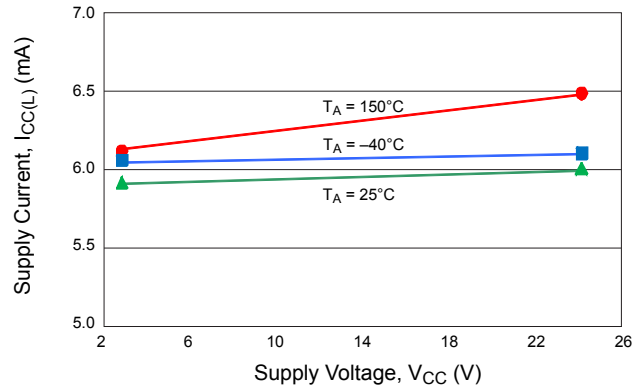


## CHARACTERISTIC PERFORMANCE

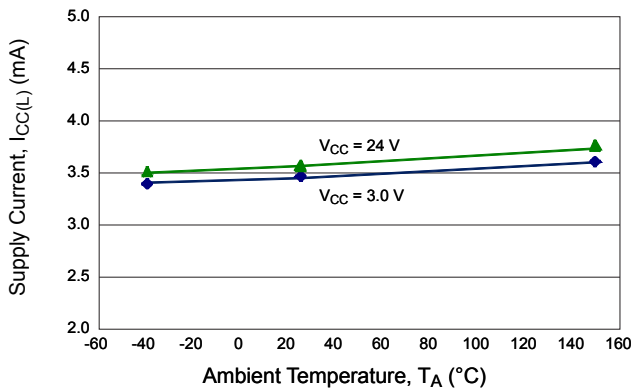
A1152/A1153/A1155/A1156  
Average Supply Current (Low) versus Temperature



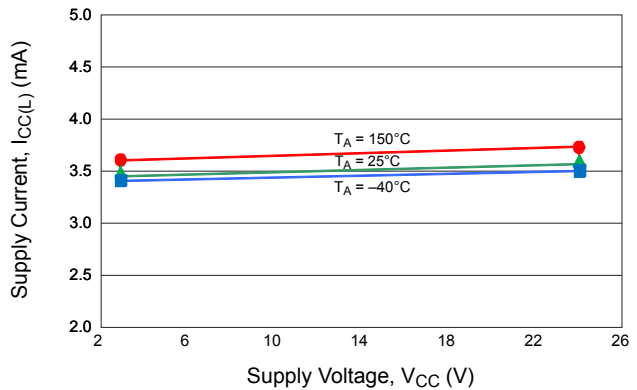
A1152/A1153/A1155/A1156  
Average Supply Current (Low) versus Supply Voltage



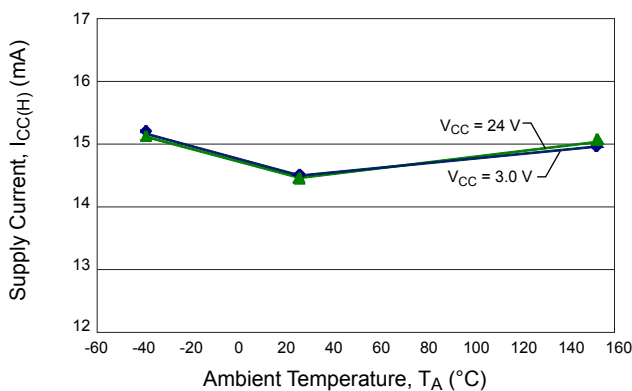
A1150/A1157/A1158  
Average Supply Current (Low) versus Temperature



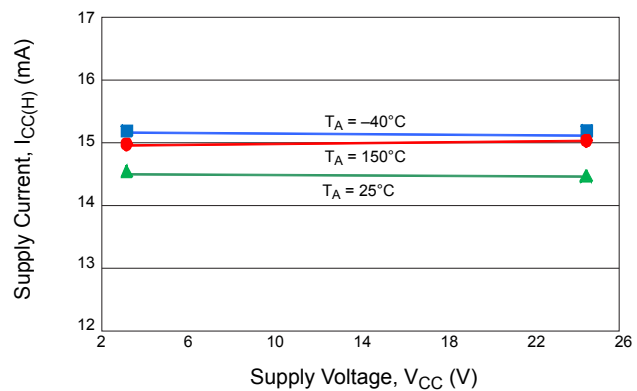
A1150/A1157/A1158  
Average Supply Current (Low) versus Supply Voltage



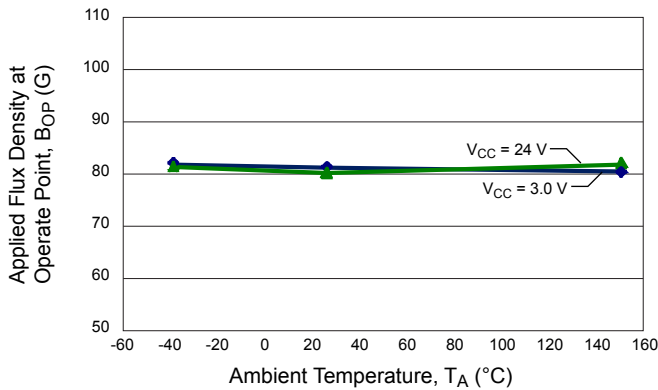
A1150/A1152/A1153/A1155/A1156/A1157/A1158  
Average Supply Current (High) versus Temperature



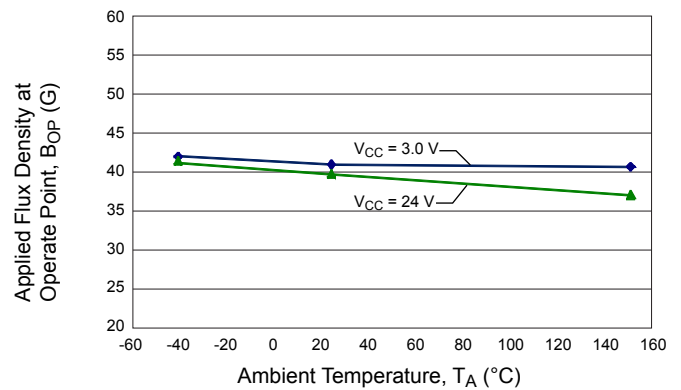
A1150/A1152/A1153/A1155/A1156/A1157/A1158  
Average Supply Current (High) versus Supply Voltage



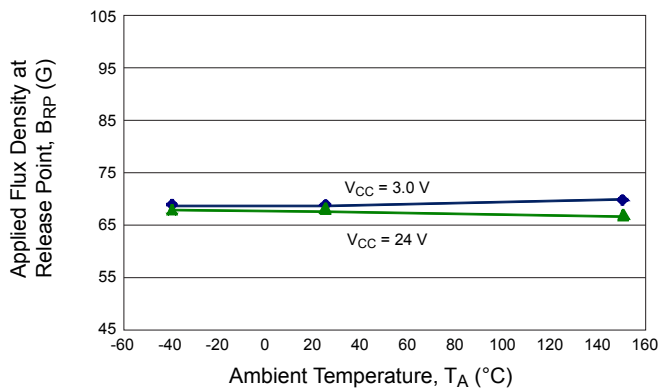
A1150/A1152/A1153  
Average Operate Point versus Temperature



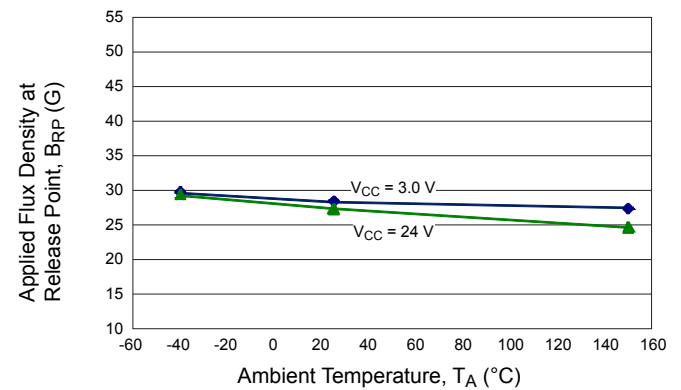
A1155/A1156  
Average Operate Point versus Temperature



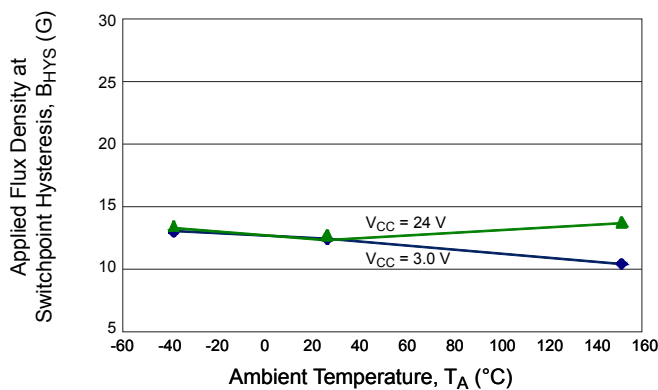
A1150/A1152/A1153  
Average Release Point versus Temperature



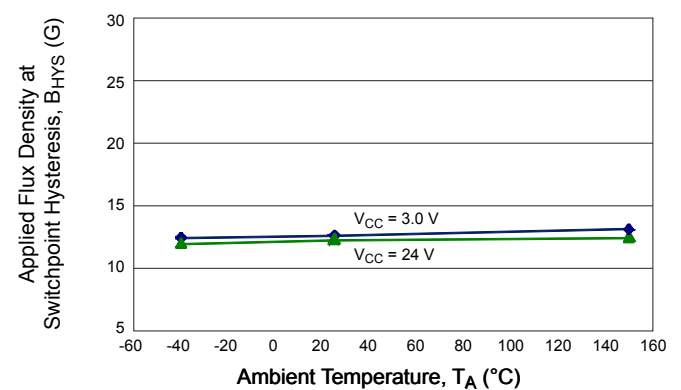
A1155/A1156  
Average Release Point versus Temperature



A1150/A1152/A1153  
Average Switchpoint Hysteresis versus Temperature



A1155/A1156  
Average Switchpoint Hysteresis versus Temperature



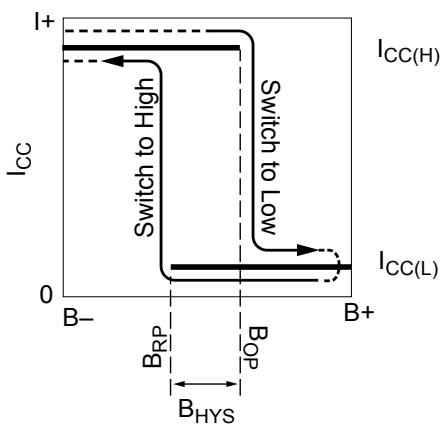
## FUNCTIONAL DESCRIPTION

The A1150, A1152, A1155, and A1157 output,  $I_{CC}$ , switches low after the magnetic field at the Hall sensor IC exceeds the operate point threshold,  $B_{OP}$ . When the magnetic field is reduced to below the release point threshold,  $B_{RP}$ , the device output goes high. This is shown in Figure 1, panel A.

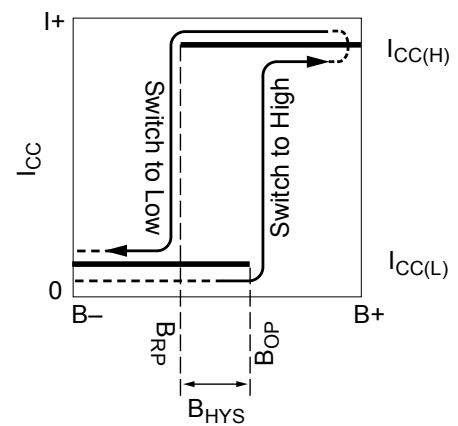
In the case of the reverse output polarity, as in the A1153, A1156, and A1158, the device output switches high after the magnetic

field at the Hall sensor IC exceeds the operate point threshold,  $B_{OP}$ . When the magnetic field is reduced to below the release point threshold,  $B_{RP}$ , the device output goes low (panel B).

The difference between the magnetic operate and release points is called the hysteresis of the device,  $B_{HYS}$ . This built-in hysteresis allows clean switching of the output even in the presence of external mechanical vibration and electrical noise.



(A) Hysteresis curve for A1150, A1152, A1155, and A1157



(B) Hysteresis curve for A1153, A1156, and A1158

**Figure 1: Alternative Switching Behaviors Available in the A115x Device Family.**

On the horizontal axis, the B+ direction indicates increasing south polarity magnetic field strength, and the B- direction indicates decreasing south polarity field strength (including the case of increasing north polarity).

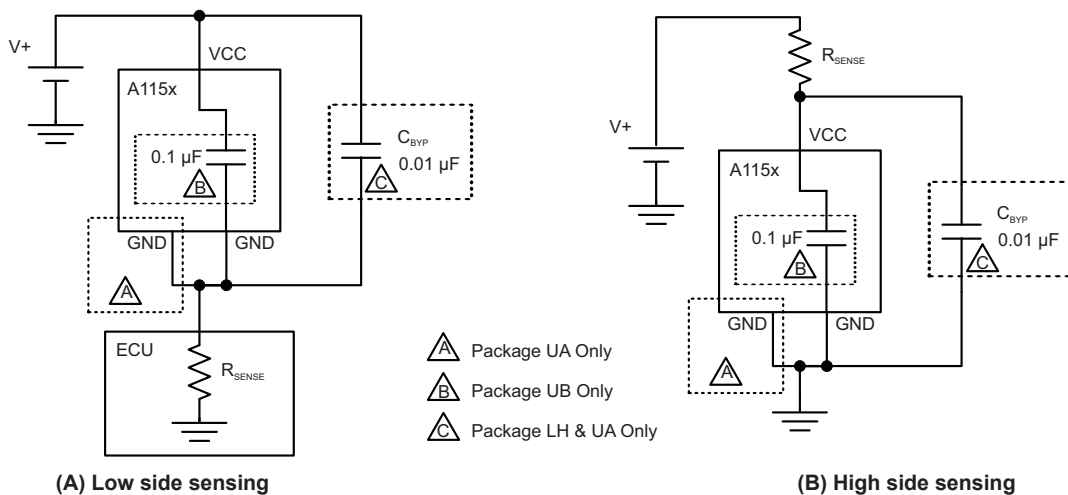


**Figure 2: Typical Application Circuits**



## Chopper Stabilization Technique

When using Hall-effect technology, a limiting factor for switchpoint accuracy is the small signal voltage developed across the Hall element. This voltage is disproportionately small relative to the offset that can be produced at the output of the Hall sensor IC. This makes it difficult to process the signal while maintaining an accurate, reliable output over the specified operating temperature and voltage ranges. Chopper stabilization is a unique approach used to minimize Hall offset on the chip. The Allegro technique, namely Dynamic Quadrature Offset Cancellation, removes key sources of the output drift induced by thermal and mechanical stresses. This offset reduction technique is based on a signal modulation-demodulation process. The undesired offset signal is separated from the magnetic field-induced signal in the frequency domain, through modulation. The subsequent demodulation acts as a modulation process for the offset, causing the magnetic field-induced signal to recover its original spectrum

at base band, while the DC offset becomes a high-frequency signal. The magnetic-sourced signal then can pass through a low-pass filter, while the modulated DC offset is suppressed. The chopper stabilization technique uses a 350 kHz high frequency clock. For demodulation process, a sample and hold technique is used, where the sampling is performed at twice the chopper frequency. This high-frequency operation allows a greater sampling rate, which results in higher accuracy and faster signal-processing capability. This approach desensitizes the chip to the effects of thermal and mechanical stresses, and produces devices that have extremely stable quiescent Hall output voltages and precise recoverability after temperature cycling. This technique is made possible through the use of a BiCMOS process, which allows the use of low-offset, low-noise amplifiers in combination with high-density logic integration and sample-and-hold circuits.

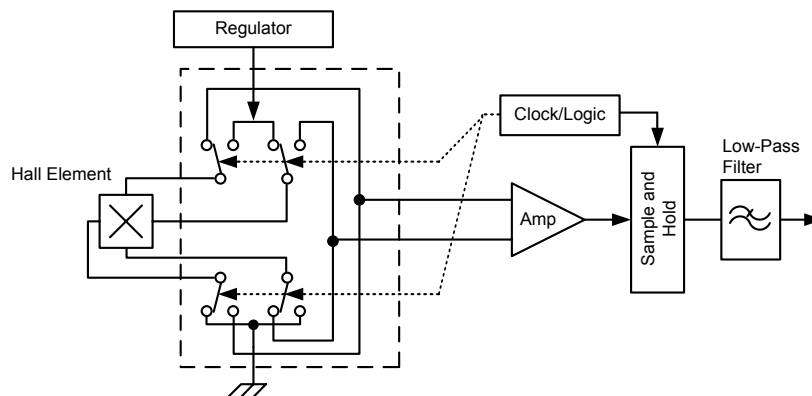


Figure 3: Chopper Stabilization Circuit (Dynamic Quadrature Offset Cancellation)

## Power Derating

The device must be operated below the maximum junction temperature of the device,  $T_J(\text{max})$ . Under certain combinations of peak conditions, reliable operation may require derating supplied power or improving the heat dissipation properties of the application. This section presents a procedure for correlating factors affecting operating  $T_J$ . (Thermal data is also available on the Allegro MicroSystems website.)

The Package Thermal Resistance,  $R_{\theta JA}$ , is a figure of merit summarizing the ability of the application and the device to dissipate heat from the junction (die), through all paths to the ambient air. Its primary component is the Effective Thermal Conductivity,  $K$ , of the printed circuit board, including adjacent devices and traces. Radiation from the die through the device case,  $R_{\theta JC}$ , is relatively small component of  $R_{\theta JA}$ . Ambient air temperature,  $T_A$ , and air motion are significant external factors, damped by overmolding.

The effect of varying power levels (Power Dissipation,  $P_D$ ), can be estimated. The following formulas represent the fundamental relationships used to estimate  $T_J$ , at  $P_D$ .

$$P_D = V_{IN} \times I_{IN} \quad (1)$$

$$\Delta T = P_D \times R_{\theta JA} \quad (2)$$

$$T_J = T_A + \Delta T \quad (3)$$

For example, given common conditions such as:  $T_A = 25^\circ\text{C}$ ,  $V_{CC} = 12\text{ V}$ ,  $I_{CC} = 4\text{ mA}$ , and  $R_{\theta JA} = 140\text{ }^\circ\text{C/W}$ , then:

$$P_D = V_{CC} \times I_{CC} = 12\text{ V} \times 4\text{ mA} = 48\text{ mW}$$

$$\Delta T = P_D \times R_{\theta JA} = 48\text{ mW} \times 140\text{ }^\circ\text{C/W} = 7^\circ\text{C}$$

$$T_J = T_A + \Delta T = 25^\circ\text{C} + 7^\circ\text{C} = 32^\circ\text{C}$$

A worst-case estimate,  $P_D(\text{max})$ , represents the maximum allowable power level ( $V_{CC}(\text{max})$ ,  $I_{CC}(\text{max})$ ), without exceeding  $T_J(\text{max})$ , at a selected  $R_{\theta JA}$  and  $T_A$ .

*Example:* Reliability for  $V_{CC}$  at  $T_A = 150^\circ\text{C}$ , package UA, using a low-K PCB.

Observe the worst-case ratings for the device, specifically:  $R_{\theta JA} = 165\text{ }^\circ\text{C/W}$ ,  $T_J(\text{max}) = 165^\circ\text{C}$ ,  $V_{CC}(\text{max}) = 24\text{ V}$ , and  $I_{CC}(\text{max}) = 17\text{ mA}$ .

Calculate the maximum allowable power level,  $P_D(\text{max})$ . First, invert equation 3:

$$\Delta T_{\text{max}} = T_J(\text{max}) - T_A = 165^\circ\text{C} - 150^\circ\text{C} = 15^\circ\text{C}$$

This provides the allowable increase to  $T_J$  resulting from internal power dissipation. Then, invert equation 2:

$$P_D(\text{max}) = \Delta T_{\text{max}} \div R_{\theta JA} = 15^\circ\text{C} \div 165\text{ }^\circ\text{C/W} = 91\text{ mW}$$

Finally, invert equation 1 with respect to voltage:

$$V_{CC(\text{est})} = P_D(\text{max}) \div I_{CC}(\text{max}) = 91\text{ mW} \div 17\text{ mA} = 5\text{ V}$$

The result indicates that, at  $T_A$ , the application and device can dissipate adequate amounts of heat at voltages  $\leq V_{CC(\text{est})}$ .

Compare  $V_{CC(\text{est})}$  to  $V_{CC}(\text{max})$ . If  $V_{CC(\text{est})} \leq V_{CC}(\text{max})$ , then reliable operation between  $V_{CC(\text{est})}$  and  $V_{CC}(\text{max})$  requires enhanced  $R_{\theta JA}$ . If  $V_{CC(\text{est})} \geq V_{CC}(\text{max})$ , then operation between  $V_{CC(\text{est})}$  and  $V_{CC}(\text{max})$  is reliable under these conditions.

## PACKAGE OUTLINE DRAWINGS

### For Reference Only – Not for Tooling Use

(Reference DWG-0000628)  
Dimensions in millimeters – NOT TO SCALE  
Dimensions exclusive of mold flash, gate burrs, and dambar protrusions  
Exact case and lead configuration at supplier discretion within limits shown

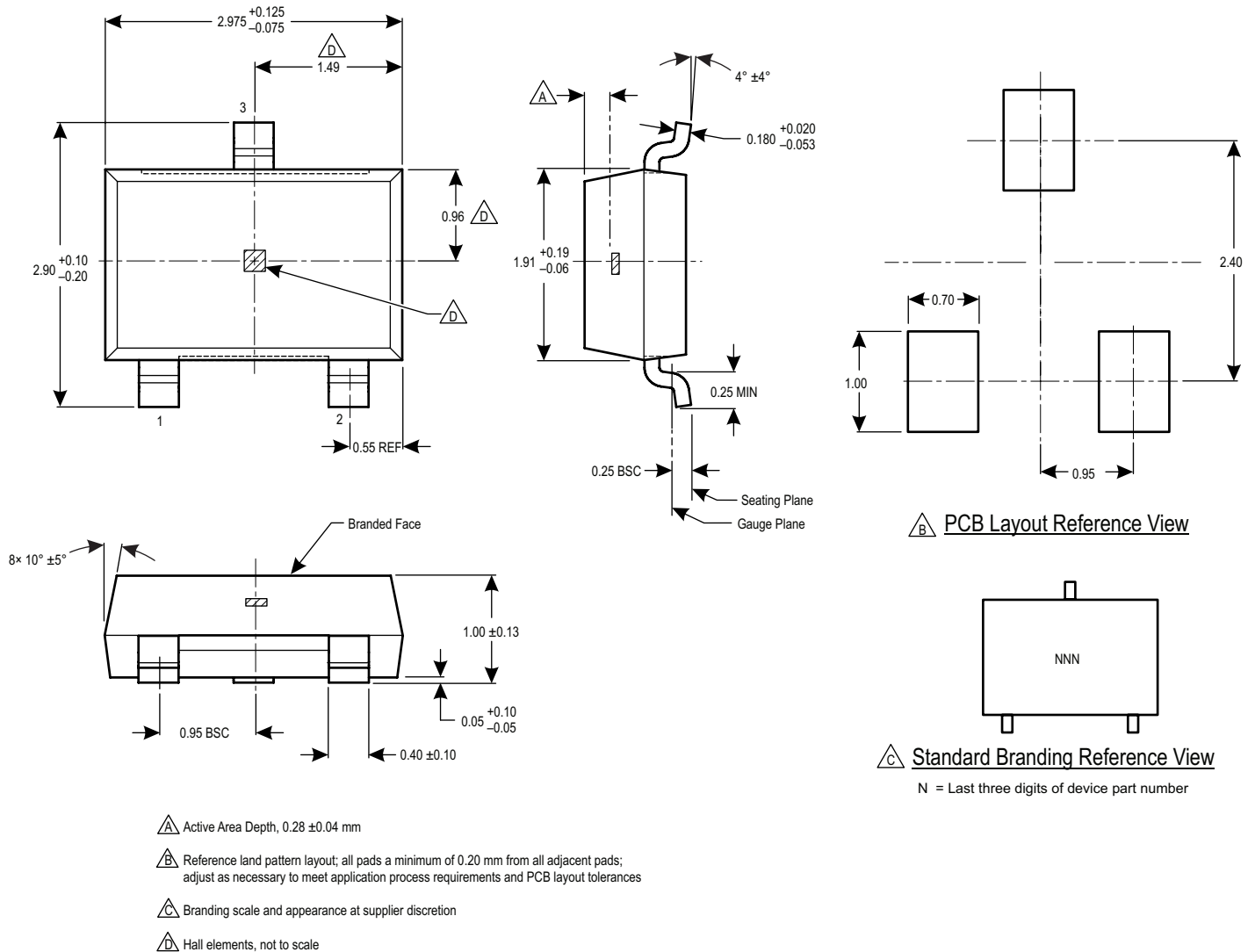


Figure 4: Package LH, 3-Pin SOT23W

## For Reference Only – Not for Tooling Use

(Reference DWG-0000404, Rev. 1)

NOT TO SCALE

Dimensions in millimeters

Dimensions exclusive of mold flash, gate burrs, and dambar protrusions  
Exact case and lead configuration at supplier discretion within limits shown

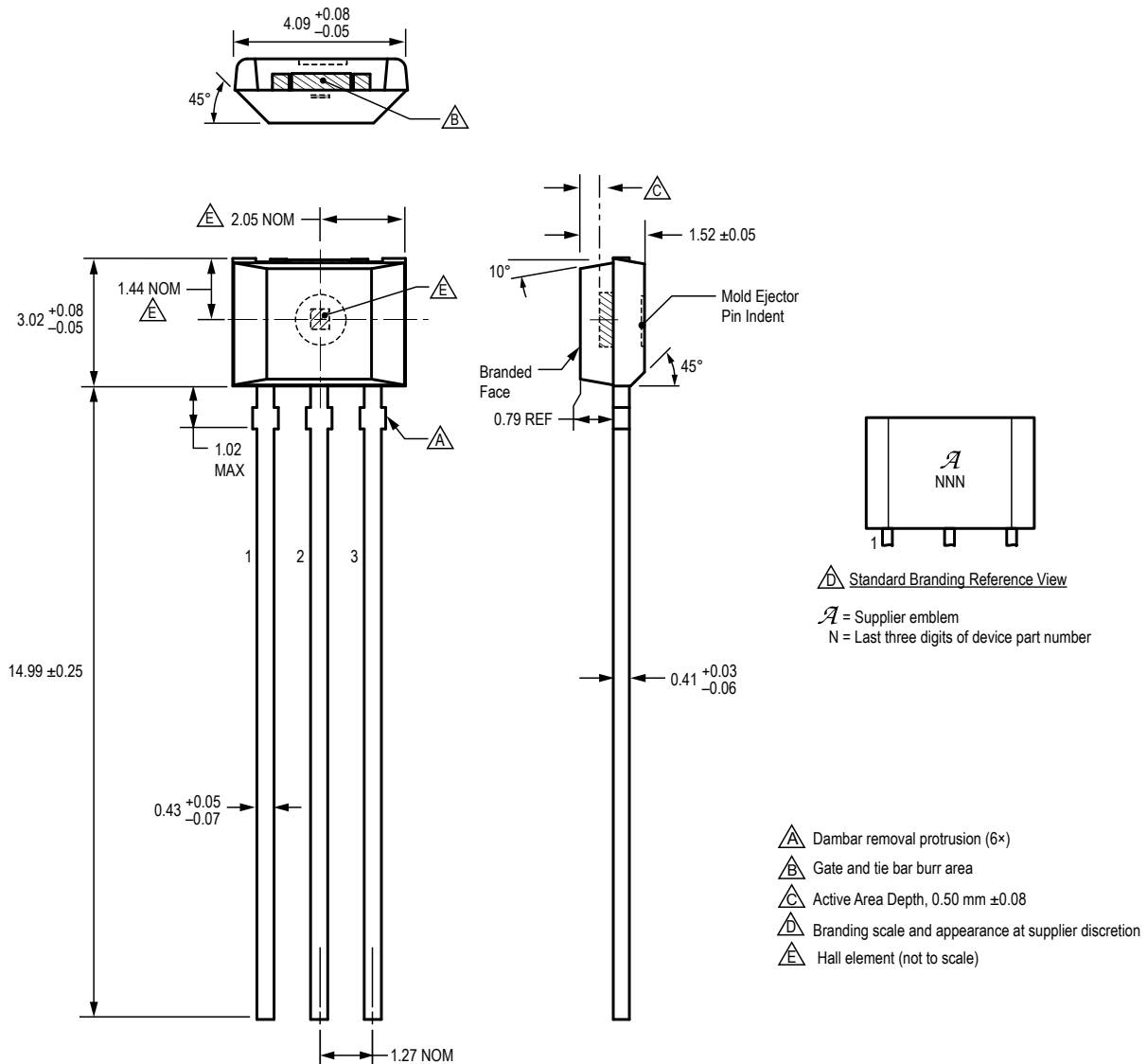


Figure 5: Package UA, 3-Pin SIP, Gate Relief



## REVISION HISTORY

Number	Date	Description
7	May 22, 2014	Added UB Package
8	October 2, 2014	Revised UB package drawing and reformatted document.
9	March 2, 2015	Updated branding info on package drawing
10	September 21, 2015	Corrected LH package Active Area Depth value; added AEC-Q100 qualification under Features and Benefits
11	August 9, 2018	Added footnote to LH package (page 3)
12	September 19, 2019	Updated LH, UA, and UB package drawings, and minor editorial updates

Copyright 2019, Allegro MicroSystems.

Allegro MicroSystems reserves the right to make, from time to time, such departures from the detail specifications as may be required to permit improvements in the performance, reliability, or manufacturability of its products. Before placing an order, the user is cautioned to verify that the information being relied upon is current.

Allegro's products are not to be used in any devices or systems, including but not limited to life support devices or systems, in which a failure of Allegro's product can reasonably be expected to cause bodily harm.

The information included herein is believed to be accurate and reliable. However, Allegro MicroSystems assumes no responsibility for its use; nor for any infringement of patents or other rights of third parties which may result from its use.

Copies of this document are considered uncontrolled documents.

For the latest version of this document, visit our website:

[www.allegromicro.com](http://www.allegromicro.com)